

## Electronic Supplementary Information

One crystal of **1-Y** was measured on an APEXII, Bruker-AXS diffractometer at Mo-K $\alpha$  radiation ( $\lambda = 0.71073 \text{ \AA}$ , graphite monochromator). The structure was solved by dual-space algorithm using the *SHELXT* program [1], and then refined with full-matrix least-squares methods based on  $F^2$  (*SHELXL*) [2]. The contribution of the disordered solvents to the calculated structure factors was estimated following the *BYPASS* algorithm [3], implemented as the *SQUEEZE* option in *PLATON* [4]. A new data set, free of solvent contribution, was then used in the final refinement. All non-hydrogen atoms were refined with anisotropic atomic displacement parameters. H atoms were finally included in their calculated positions and treated as riding on their parent atom with constrained thermal parameters.

One crystal of **1-Dy** was measured on a D8 VENTURE Bruker AXS diffractometer at Mo-K $\alpha$  radiation ( $\lambda = 0.71073 \text{ \AA}$ , multilayer monochromator). The structure was solved by dual-space algorithm using the *SHELXT* program [1], and then refined with full-matrix least-squares methods based on  $F^2$  (*SHELXL*) [2]. The contribution of the disordered solvents to the calculated structure factors was estimated following the *BYPASS* algorithm [3], implemented as the *SQUEEZE* option in *PLATON* [4]. A new data set, free of solvent contribution, was then used in the final refinement. All non-hydrogen atoms were refined with anisotropic atomic displacement parameters. Except water molecules hydrogen atoms that were introduced in the structural model through Fourier difference maps analysis, H atoms were finally included in their calculated positions and treated as riding on their parent atom with constrained thermal parameters.

- [1] G. M. Sheldrick, *Acta Cryst.* A71 (2015) 3-8  
[2] Sheldrick G.M., *Acta Cryst.* C71 (2015) 3-8  
[3] P. v.d. Sluis and A.L. Spek, *Acta Cryst.* (1990) A46, 194-201  
[4] A. L. Spek, *J. Appl. Cryst.* (2003), 36, 7-13

	<b>1-Dy</b>	<b>1-Y</b>
<b>Formula</b> -	C <sub>34</sub> H <sub>35</sub> Dy F <sub>6</sub> N <sub>5</sub> O <sub>11</sub> S <sub>2</sub> , C F <sub>3</sub> O <sub>3</sub> S, CH <sub>2</sub> Cl <sub>2</sub>	C <sub>34</sub> H <sub>35</sub> Y F <sub>6</sub> N <sub>5</sub> O <sub>11</sub> S <sub>2</sub> , CH <sub>2</sub> Cl <sub>2</sub>
<b>FW (g.mol<sup>-1</sup>)</b>	1264.28	1041.63
<b>Cryst. Syst.</b>	Trigonal	Trigonal
<b>Space group</b>	'R -3'	'R -3'
<b>a = b (Å)</b>	47.4786(14)	47.523(4)
<b>c (Å)</b>	11.5392(4)	11.523(5)
<b>α = β (°)</b>	90	90
<b>γ (°)</b>	120	120
<b>V (Å<sup>3</sup>)</b>	22526.9(10)	22482(3)
<b>Z</b>	18	18
<b>D<sub>ca</sub> (g.cm<sup>-3</sup>)</b>	1.678	1.385
<b>T (K)</b>	150(2)	150(2)
<b>R [I&gt;2σ]</b>	0.0439	0.0846
<b>R<sub>w2</sub> [I&gt;2σ]</b>	0.1223	0.2048

**Table S1:** X-Ray crystallographic details for complexes **1-Dy** and **1-Y**. Note that the squeeze procedure was used to treat disordered solvent in the case of **1-Dy** and disordered solvent and free triflate ion in the case of **1-Y**.

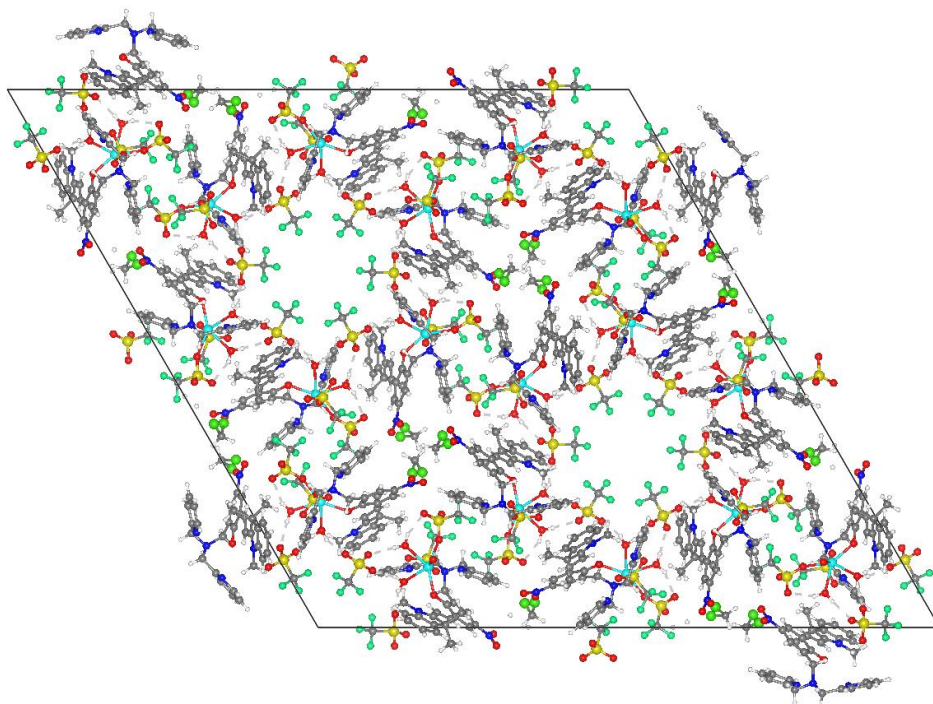


Figure S1: View of the packing of **1-Dy** in the ab plane, obtained from the XRD analysis. Grey, blue, red, yellow, green, white and light blue spheres represent C, N, O, S, F, H and Dy atoms, respectively.

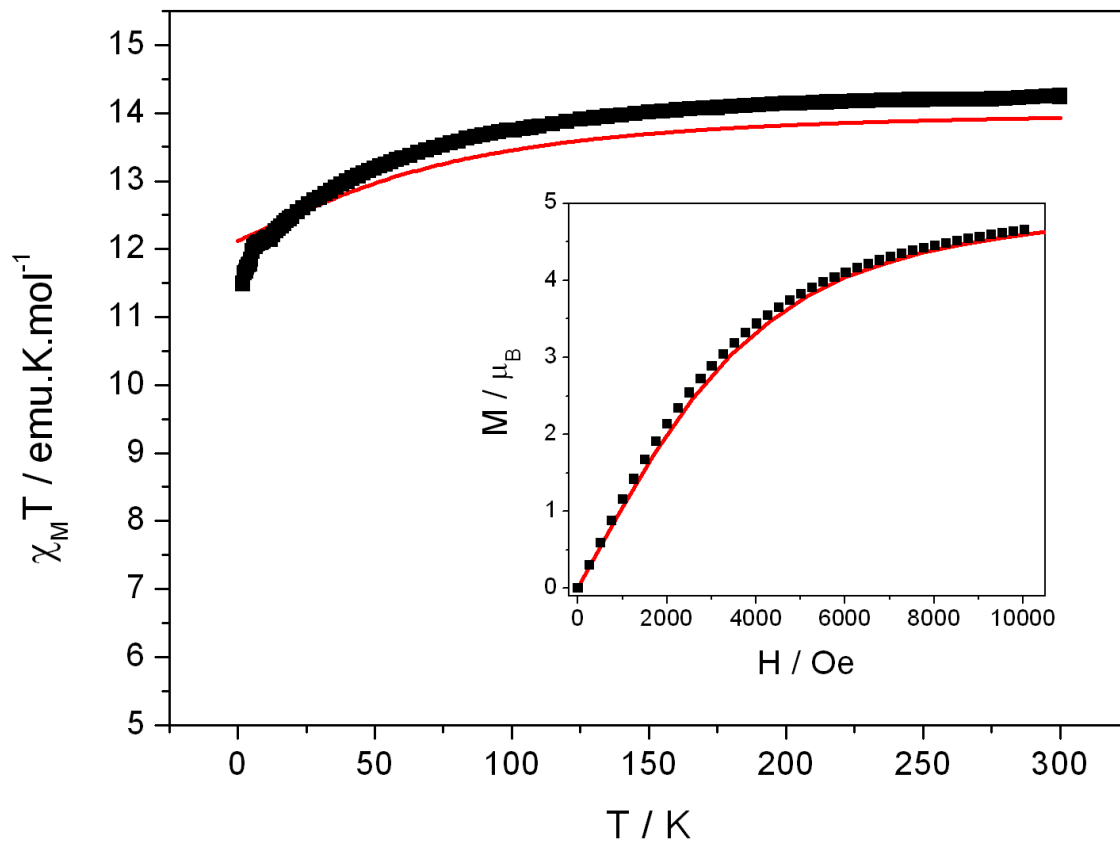


Figure S2: Temperature dependence of  $\chi_M T$  of **1-Dy<sub>solid</sub>** and simulation from ab-initio calculations. Inset: Field dependence of the magnetization **1-Dy<sub>solid</sub>** at 2K and simulation from ab-initio calculations.

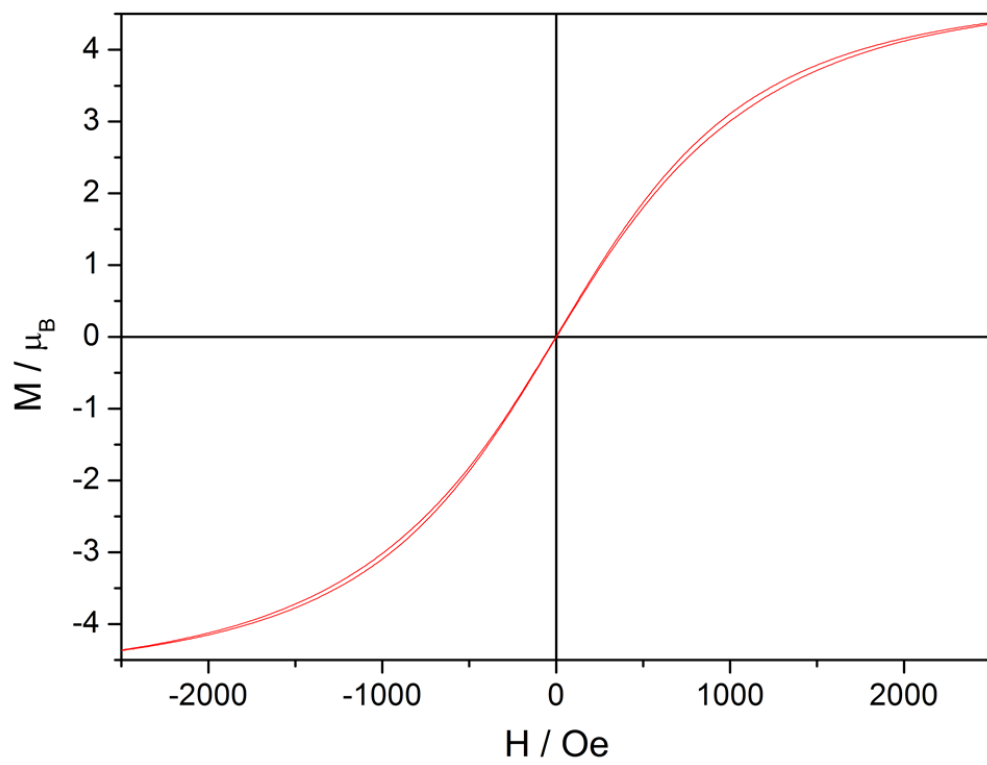


Figure S3: Hysteresis curve of  $1\text{-Dy}_{\text{solid}}$  measured at 0.47K with a field sweep rate of  $16 \text{ Oe}\cdot\text{s}^{-1}$

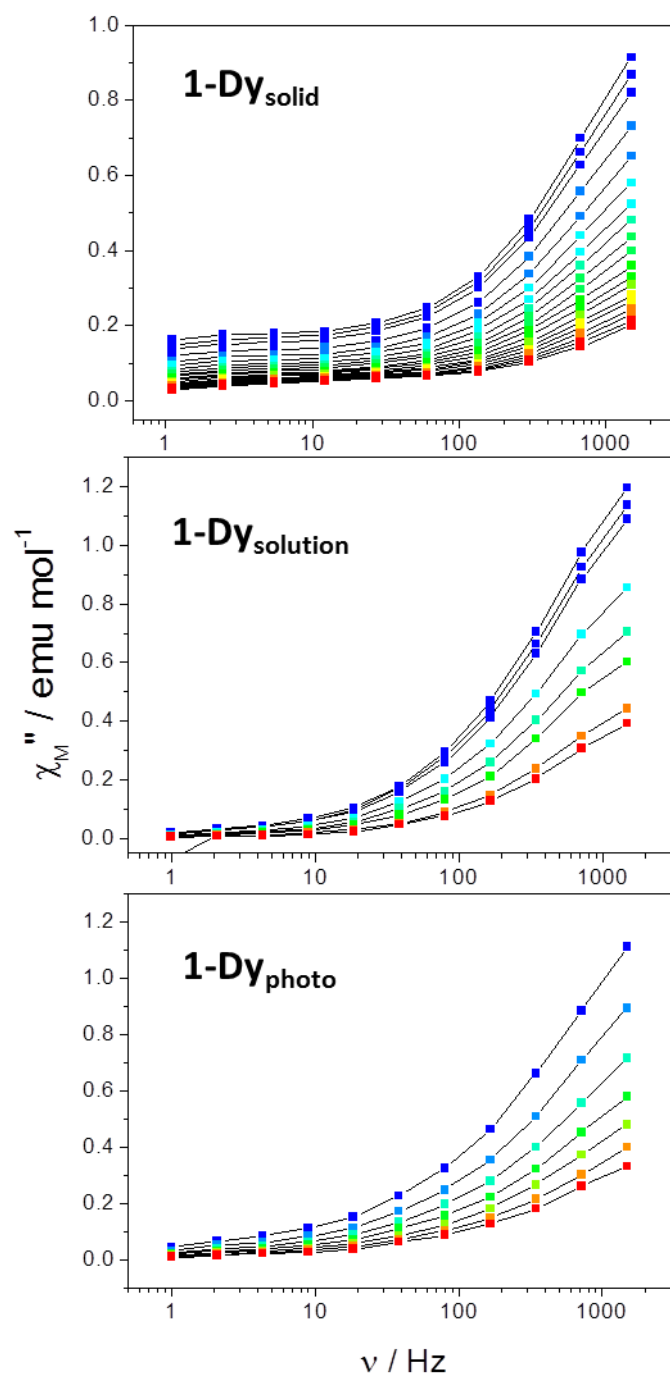


Figure S4: Frequency dependence of  $\chi_M''$  of **1-Dy<sub>solid</sub>**, **1-Dy<sub>solution</sub>** and **1-Dy<sub>photo</sub>** measured with  $H_{dc} = 0$  Oe for temperatures ranging from 1.8 K (blue) to 5 K (red). Lines are guide to the eye.

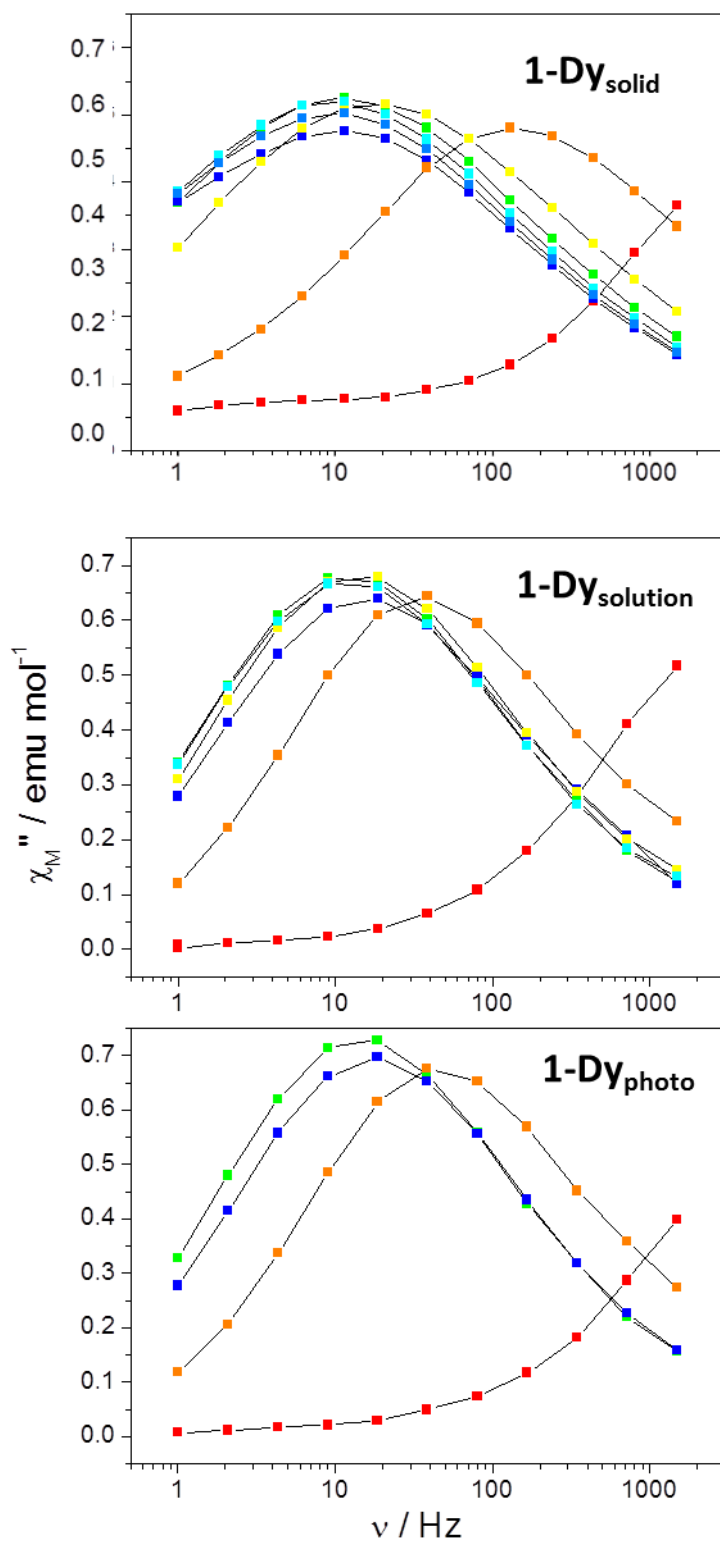


Figure S5: Frequency dependence of  $\chi_M''$  of **1-Dy<sub>solid</sub>**, **1-Dy<sub>solution</sub>** and **1-Dy<sub>photo</sub>** at 4K (top to bottom) with field from 0 Oe (red) to 2400 Oe (blue) with 300 Oe spacing. Lines are guide to the eye.

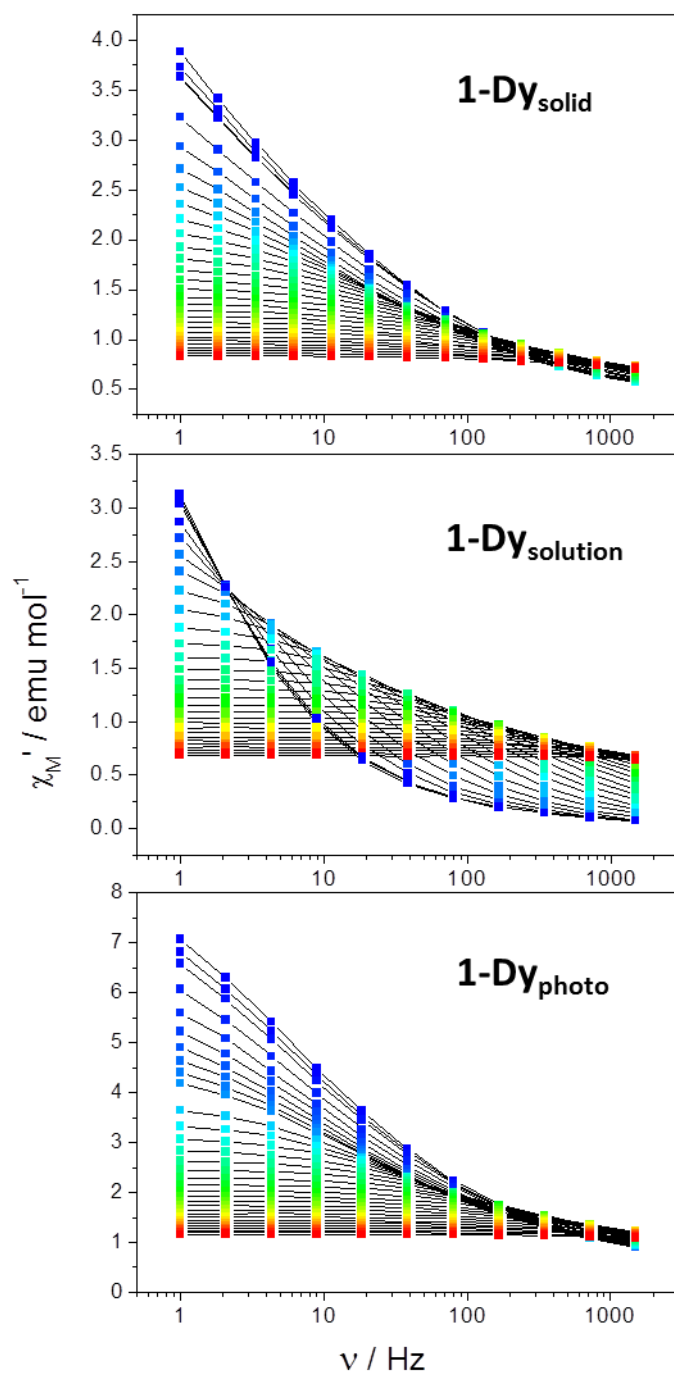


Figure S6: Frequency dependence of  $\chi_M''$  of **1-Dy<sub>solid</sub>**, **1-Dy<sub>solution</sub>** and **1-Dy<sub>photo</sub>** measured with  $H_{dc}=1200$  Oe for temperatures ranging from 2K (blue) to 15K (red). Lines are guide to the eye.

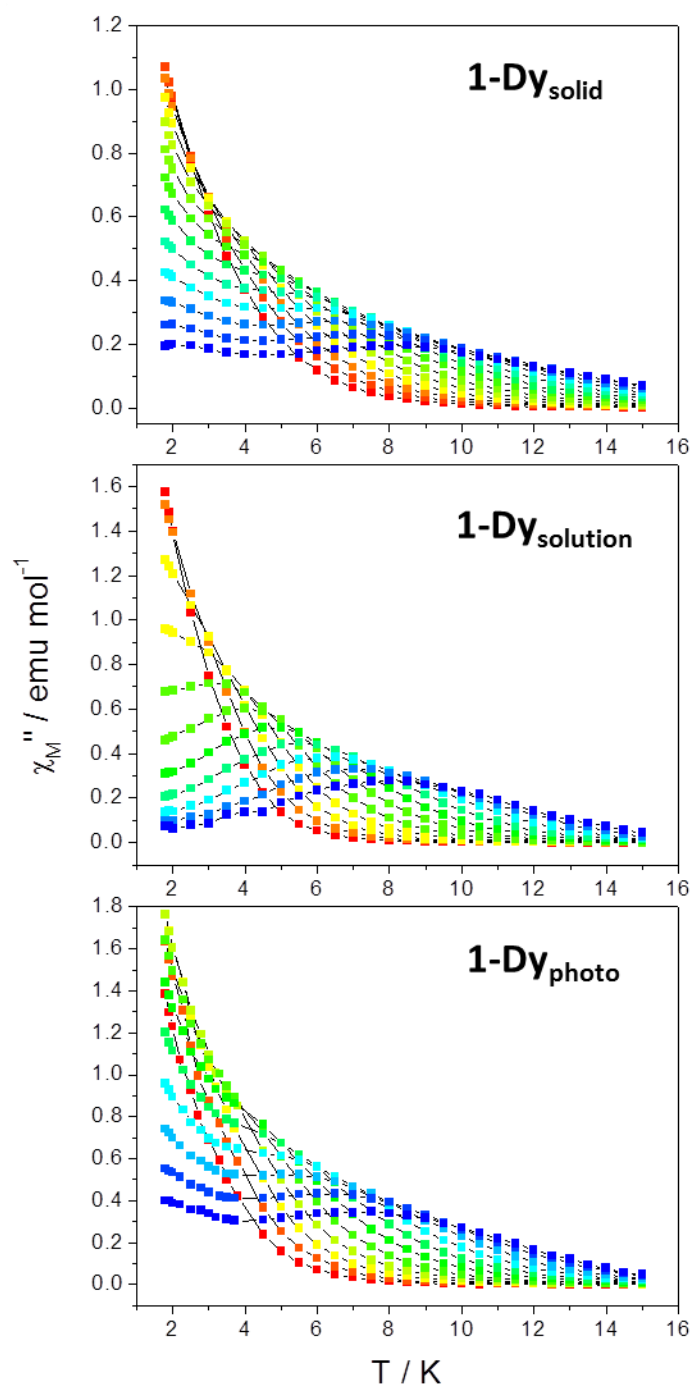


Figure S7: Temperature dependence of  $\chi_M''$  of **1-Dy<sub>solid</sub>**, **1-Dy<sub>solution</sub>** and **1-Dy<sub>photo</sub>** measured with  $H_{dc}=1200$  Oe for frequencies ranging from 1 Hz (red) to 1500 Hz (blue). Lines are guide to the eye.

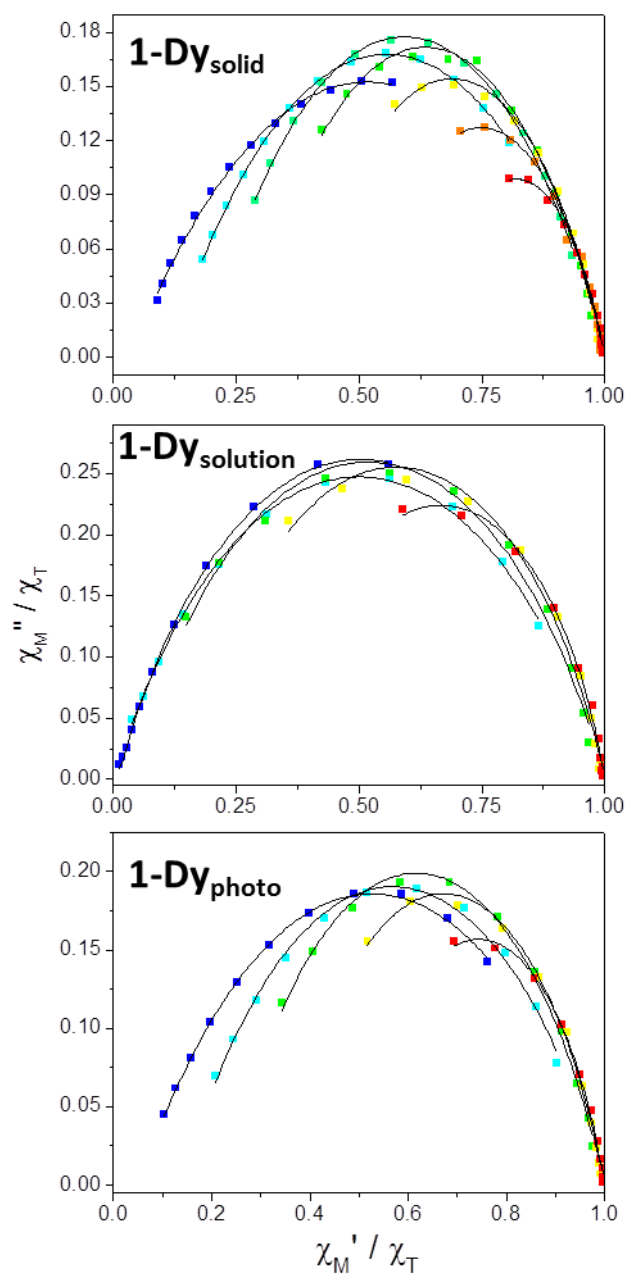


Figure S8: Argand (Cole-Cole) plots and some selected fits for **1-Dy<sub>solid</sub>**, **1-Dy<sub>solution</sub>** and **1-Dy<sub>photo</sub>** measured with  $H_{dc}=1200$  Oe for selected temperatures ranging from 2 K (blue) to 10 K (red).

Table S2: Extracted values from the fitting of  $X''$  vs frequency curves under 1200 Oe field of **1-Dy<sub>solid</sub>**

T(K)	$\tau$ ( $\mu$ s)	T(K)	$\tau$ ( $\mu$ s)
1.8	96084.56	7.5	1021.73
1.9	102399.6	8	799.17
2	100749.27	8.5	594.54
2.5	65555.84	9	473.52
3	36257.25	9.5	379.6
3.5	21709.96	10	329.27
4	13903.66	10.5	287.54
4.5	9001.14	11	254.31
5	5887.86	11.5	222.53
5.5	3960.92	12	184.9
6	2711.19	12.5	170.65
6.5	1907.88	13	164.44
7	1353.22		

Table S3: Extracted values from the Argand plot under 1200 Oe field of **1-Dy<sub>solid</sub>**

T (K)	$\chi_s$	$\chi_T$	$\alpha$	R <sup>2</sup>
1.8	0.24104	6.74066	0.59547	0.99697
1.9	0.22679	6.61493	0.60664	0.99702
2	0.2258	6.39484	0.60017	0.99729
2.5	0.24422	5.27321	0.6126	0.99813
3	0.2895	4.2785	0.5896	0.99927
3.5	0.33186	3.59548	0.5615	0.99969
4	0.35132	3.12853	0.53968	0.99974
4.5	0.36933	2.76077	0.51603	0.99953
5	0.371	2.48	0.5029	0.99958
5.5	0.37736	2.24794	0.4884	0.99885
6	0.38143	2.0599	0.47694	0.99832
6.5	0.384	1.90268	0.46954	0.9973
7	0.38312	1.7713	0.46914	0.99319
7.5	0.399	1.65112	0.45342	0.99621
8	0.41581	1.54813	0.44111	0.99504
8.5	0.4211	1.4574	0.44035	0.99509
9	0.43326	1.37682	0.4321	0.99546
9.5	0.44717	1.30599	0.42633	0.99514
10	0.46948	1.24207	0.41361	0.99585
10.5	0.48938	1.18334	0.40483	0.99596
11	0.5079	1.1302	0.3942	0.99619
11.5	0.51832	1.08265	0.38992	0.99649
12	0.51214	1.03252	0.40479	0.99119
12.5	0.54784	0.99278	0.36998	0.99617
13	0.56059	0.95661	0.3597	0.99612
13.5	0.56146	0.92324	0.36467	0.9959
14	0.57109	0.89229	0.36147	0.99523
14.5	0.57884	0.8627	0.3546	0.99545
15	0.59261	0.83505	0.3444	0.99658

Table S4: Extracted values from the fitting of  $X''$  vs frequency curves under 1200 Oe field of **1-Dy**<sub>solution</sub>

T(K)	$\tau$ ( $\mu$ s)	T(K)	$\tau$ ( $\mu$ s)
1.8	143450.04376	6	1503.42543
1.9	131081.88343	6.5	1007.80015
2	118698.34227	7	719.47591
2.5	71002.95228	7.5	511.9609
3	40467.11818	8	384.37814
3.5	21854.94094	8.5	290.81952
4	12196.32838	9	233.64628
4.5	6868.09025	9.5	183.65093
5	3877.63302	10	160.39495
5.5	2369.11794		

Table S5: Extracted values from the Argand plot under 1200 Oe field of **1-Dy**<sub>solution</sub>

T (K)	$\chi_s$	$\chi_T$	$\alpha$	R <sup>2</sup>
1.8	0.04431	5.96841	0.37437	0.99964
1.9	0.03479	5.71858	0.38253	0.99939
2	0.03559	5.42408	0.38303	0.9997
2.5	0.02037	4.41179	0.40227	0.99985
3	0.01543	3.69211	0.40693	0.99965
4	0.00224	2.77965	0.41499	0.99756
4.5	0.03539	2.42977	0.39305	0.99682
5	0.02462	2.17785	0.39364	0.99283
5.5	0.04867	1.96565	0.37717	0.98823
6	0.06396	1.78769	0.37161	0.98415
6.5	0.09239	1.64132	0.35483	0.98651
7	0.12855	1.51655	0.33758	0.98793
7.5	0.15997	1.41119	0.32476	0.99043
8	0.19886	1.31954	0.31108	0.99125
8.5	0.24031	1.23594	0.28906	0.99154
9	0.27899	1.1635	0.27887	0.99119
9.5	0.31085	1.10116	0.26615	0.99061
10	0.34595	1.04271	0.2483	0.9947

Table S6: Extracted values from the fitting of  $X''$  vs frequency curves under 1200 Oe field **1-Dy<sub>photo</sub>**

T(K)	$\tau$ ( $\mu$ s)	T(K)	$\tau$ ( $\mu$ s)
1.8	23891.64684	5	2483.05791
1.9	22926.70661	5.5	1676.17778
2	22375.01916	6	1178.30995
2.25	20418.43954	6.5	838.62261
2.5	17682.37781	7	621.9
2.75	15026.57376	7.5	465.3299
3	12762.16544	8	357.88766
3.25	10681.60089	8.5	279.52919
3.5	8772.402	9	214.07418
3.75	7096.22103	9.5	190.4379
4	5714.96181	10	155.29641
4.5	3835.38525		

Table S7: Extracted values from the Argand plot under 1200 Oe field of **1-Dy<sub>photo</sub>**

T (K)	$\chi_s$	$\chi_T$	$\alpha$	R <sup>2</sup>
1.8	0.43191	9.36057	0.51867	0.99981
1.9	0.43872	8.96676	0.52102	0.99965
2	0.44582	8.63589	0.52492	0.99892
2.5	0.49941	7.11174	0.52628	0.99915
3	0.53038	5.95328	0.51645	0.99418
3.5	0.58371	5.07573	0.49391	0.99079
4	0.60278	4.40776	0.47152	0.99572
4.5	0.62667	3.91881	0.44965	0.99612
5	0.64001	3.49759	0.42886	0.99079
5.5	0.65017	3.17212	0.41155	0.99713
6	0.67306	2.90005	0.3918	0.99417
6.5	0.69023	2.67473	0.37949	0.99779
7	0.71638	2.47965	0.36161	0.99602
7.5	0.72926	2.31604	0.35418	0.99885
8	0.74631	2.17169	0.34437	0.99643
8.5	0.77511	2.03932	0.32621	0.99855
9	0.78060	1.92858	0.32844	0.99663
9.5	0.81975	1.82661	0.31666	0.99929
10	0.84427	1.73652	0.30292	0.997
10.5	0.85731	1.65346	0.30252	0.99821
11	0.88144	1.57906	0.2952	0.99588

**Table S8:** Computed energies levels (the ground state is set at zero), component values of the Lande factor  $g$  and wavefunction composition for each  $M_J$  state of the ground-state multiplet for **1-Dy**.

	Energy (cm <sup>-1</sup> )	$g_x$	$g_y$	$g_z$	Wavefunction composition <sup>a</sup>
1	0.0	0.00	0.00	19.69	0.98   $\pm 15/2$ >
2	137.9	0.22	0.24	16.56	0.83   $\pm 13/2$ >
3	215.7	1.56	1.98	13.21	0.32   $\pm 11/2$ > + 0.20   $\pm 9/2$ > + 0.18   $\pm 1/2$ >
4	258.5	1.77	4.75	11.14	0.24   $\pm 7/2$ > + 0.21   $\pm 11/2$ > + 0.18   $\pm 3/2$ > + 0.17   $\pm 5/2$ > + 0.11   $\pm 1/2$ >
5	308.9	2.21	4.31	11.46	0.30   $\pm 5/2$ > + 0.24   $\pm 3/2$ > + 0.17   $\pm 11/2$ > + 0.13   $\pm 1/2$ >
6	352.2	1.41	3.37	13.49	0.44   $\pm 1/2$ > + 0.23   $\pm 3/2$ > + 0.19   $\pm 9/2$ >
7	394.8	0.42	1.20	18.17	0.22   $\pm 3/2$ > + 0.21   $\pm 5/2$ > + 0.20   $\pm 7/2$ > + 0.18   $\pm 9/2$ > + 0.13   $\pm 1/2$ >
8	455.0	0.12	0.29	19.18	0.33   $\pm 7/2$ > + 0.25   $\pm 9/2$ > + 0.20   $\pm 5/2$ > + 0.13   $\pm 11/2$ >

<sup>a</sup> Only the contributions > 10% are given.